duction to less than 1 kilogram a year.

To the surprise of many, Iranian officials have—in principle—agreed to even more stringent changes. Not only will Arak switch to LEU fuel, but engineers will also downsize the reactor's calandria—the vessel in which the fuel resides—because LEU fuel requires less space. That downsizing also would make it harder to restore natural uranium fuel to the reactor and produce more plutonium. The changes would lengthen the plutonium breakout time to several years, Moniz estimates. And even that could be a moot point: Iran has pledged to ship all of Arak's spent fuel out of the country for the reactor's lifetime, Moniz says.

An Arak redesign will be worked out in the coming weeks. "They want and we want the P5+1 to certify the redesign," Moniz says. Besides minimizing plutonium production, the new design would increase the reactor's neutron flux—which would make it more efficient at generating medical radioisotopes and "would be good for their research program," Moniz says. Siegfried Hecker, a plutonium specialist at Stanford University in Palo Alto, California, and former director of Los Alamos National Laboratory, has called for developing Arak as an international user facility for medicine and materials science. Although that idea is not in the draft agreement, Moniz says "it's still on the table."

The notion of making the Arak reactor an international facility "is still on the table."

Ernest Moniz, U.S. energy secretary

Fordow, however, would become what Moniz terms an "international physics center." The facility would be largely gutted, with about two-thirds of its centrifuges removed. The remaining 1044 centrifuges, Moniz says, would be modified to produce molybdenum (Mo) and iridium (Ir) isotopes for use in medicine and engineering. In molybdenum's case, the goal would be to increase the proportion of the isotope Mo-98 in samples, then expose them to neutrons at Arak to make Mo-99. Mo-99 is the parent of technetium-99m, a radioisotope used in more than 20 million nuclear medicine procedures a year. The other enrichment target is Ir-191; adding a neutron makes Ir-192, which is widely used in gamma cameras to check for structural flaws in metal. As a nonproliferation dividend, the modified centrifuges would become so contaminated with isotopes that "those machines would be very much unusable" for making weapons-grade uranium, says a U.S. official.

Each of the P5+1 nations is seeking to carve out other research niches at Fordow. French negotiators have even floated the idea of installing up to three low-energy electron linear accelerators. "The concept is an accelerator center of excellence," says the U.S. official. Opening up Fordow "is a great idea to get [Iran] into the international research community," Hecker adds.

Several other facets of the deal are also aimed at blocking the uranium pathways to a bomb. For starters, Iran would reduce the number of installed centrifuges for enriching uranium from about 19,000 to 5060—all of which, for at least 10 years, would be Iran's less capable, first-generation IR-1 centrifuges. Iran would also soon end research projects involving its more advanced IR-2m and IR-4 centrifuges, which "will be removed and put under seal," Moniz says. And the country's LEU stockpile would be slashed from about 10,000 kilograms to 300 kilograms.

One option for achieving that reduction is to blend the LEU with depleted uranium, which, compared with natural uranium, contains less of the fissile isotope uranium-235. But Frank von Hippel, a physicist and arms control expert at Princeton University in New Jersey, says that approach would "throw away all the enrichment work"—a waste of valuable reactor fuel. A more logical solution, he says, would be to send the excess LEU to Russia for conversion into fuel rods for Iran's Bushehr nuclear reactor, in operation since 2011.

The "single biggest challenge," Acton says, will be eliminating the covert pathway. To improve the odds of detecting secret work, the final agreement will detail an intrusive inspection regime and unprecedented oversight of Iran's purchases for its nuclear program.

Other thorny issues remain. One is Iran's R&D on laser enrichment of uranium, a new route to fissile material that could be even easier to hide than ranks of centrifuges. "That's not something we want to see them pursuing," says the U.S. official. And Acton says it's worth bearing in mind that, until negotiators hammer out the final details, "we don't have a deal." ■

PHOTO: AP PHOTO/RONALD ZAK

GEOCHEMISTRY

Acid oceans cited in Earth's worst die-off

Signature of acidification found in Permian extinctions 250 million years ago

By **Eric Hand**

Things went really sour for life on Earth 250 million years ago. A team of European geoscientists has found the most direct evidence yet that the world's oceans became sharply acidic at the boundary between the Permian and Triassic periods—when scientists estimate 90% of Earth's species died in the worst mass extinction ever.

The "PT" die-off affected all types of living things, but it hit marine species the hardest—killing off, for instance, the once-ubiquitous trilobites. The new study, published on page 229 of this issue, concludes that the ocean acidification played a major role in the cataclysm. Acidification can kill sea creatures by weakening their ability to produce their calcium-bearing shells, and it is driven by excess carbon dioxide (CO_2) dissolving in the ocean. As such, the extinction holds a cautionary lesson for today: Because of CO_2 released by burning fossil fuels, oceans could now be acidifying even faster than they did 250 million years ago, although the process hasn't yet persisted nearly as long.

"It's not inconsequential that we are disrupting the earth's carbon cycle at a faster rate than the worst extinction of all time," says Lee Kump, a geochemist at Pennsylvania State University, University Park. "Even if it only exists for a few centuries rather than 10,000 years, rates of change do matter."

Unlike the asteroid-induced extinction that killed the dinosaurs 66 million years ago, most scientists think the even bigger catastrophe at the end of the Permian was homegrown: triggered by a massive bout of volcanism in Siberia that released trillions of tons of carbon into the atmosphere and oceans. Researchers previously found signs that living things endured multiple stresses as a result of the eruptions: global warming, ocean acidification, a drop in dissolved oxygen in the oceans, and even a buildup

of toxic sulfur. But sorting out the relative importance and interdependence of these effects has been difficult.

Now, scientists have better evidence that ocean acidification hit living things hard. It comes from carbonate-bearing limestones in the United Arab Emirates. They formed some 250 million years ago in the shallow waters offshore of Pangaea, the supercontinent at the time, locking in the geochemical signals of the ancient Tethys Ocean. Traditionally, geochemists have used variations in certain carbon isotopes as a sign that a pulse of atmospheric carbon dioxide was entering the ocean and triggering acidification. But in the new *Science* study, researchers analyzed the Tethys rocks for isotopes of boron—a fainter signal, but one that corresponds more directly to ocean acidity. The method works because chemical reactions in seawater cause the ratio of the isotope boron-11 to boron-10 to increase along with the pH. Rocks that precipitate on the sea floor reflect those changing ratios—and with them, the changing acidity of the ocean over time.

The researchers found a drop in the isotopic signal that would have corresponded to a drop of 0.6 to 0.7 pH units—a significant change in seawater chemistry. "This is the first really direct evidence of ocean acidification for this mass extinction," says Matthew Clarkson, a geochemist at the University of Otago, Dunedin, in New Zealand, who led the study.

The boron anomaly comes about 50,000 years after a sharp change in carbon isotopes that has long been thought to signal the start of ocean acidification and the beginning of the extinction. The study team says the gap between the carbon and boron signals suggests that separate pulses from carbon-spewing volcanoes drove a two-stage extinction, an idea first put forward in 2012. First, a slow 50,000-year pulse of carbon entered the air and then the oceans. The researchers hypothesize that the oceans were already somewhat alkaline, allowing them to absorb the incoming CO_2 with very little change in pH and modest impacts on marine life. But then a second, sharper pulse of carbon arrived in a period of 10,000 years, overwhelming the oceans' feedback mechanisms.

Musandam mountain cliffs in the United Arab Emirates include rocks laid down during a 250-million-year-old catastrophe that killed off 90% of life on Earth.

Clarkson says the scenario explains why paleontologists have found that sea animals like gastropods and bivalves—calcifying creatures that are most susceptible to acidification—suffered their greatest losses in the later stage of the Permian extinction. "The fossil record supports what we're seeing with the geochemistry," he says. Andrew Knoll, a paleontologist at Harvard University, agrees that a late, sharp pulse of acidification could help explain the extinction record.

The Permian-Triassic catastrophe holds mixed messages for Earth today. On the one hand, the pace of acidification was slower than it is now. The study team estimates that, in the acidification event, 24,000 gigatons of carbon were injected into the atmosphere over 10,000 years—a rate of 2.4 gigatons per year—and most of it wound up in the oceans. Currently, scientists estimate carbon from all sources is entering the atmosphere at a rate of about 10 gigatons per year.

On the other hand, today's economically viable fossil fuel reserves contain only about 3000 gigatons of carbon—far shy of the Permian total, even if human beings burn it all. "We're injecting the carbon faster, but it's unlikely that we have as much carbon to inject," says study co-author Tim Lenton, an Earth systems scientist at the University of Exeter in the United Kingdom. But knowing that the Permian was much worse doesn't bring Lenton much comfort. "Biology is pretty smart—it can cope with a certain amount of acidification," he says. "But I suspect there are limits to adaptation. There will be some point at which [species] crack."

Study co-author Rachel Wood, a geobiologist at the University of Edinburgh in the United Kingdom, wants to make sure that the acidification pulse was more than a regional catastrophe. The team next plans to test rocks that formed on the floor of the Tethys 250 million years ago in present-day Iran and Oman. "We need to establish that this is a global signature," she says. ■

Acid bath

The rocks that recorded the deadly ocean acidification were once the floor of a shallow sea off the coast of the supercontinent Pangaea.

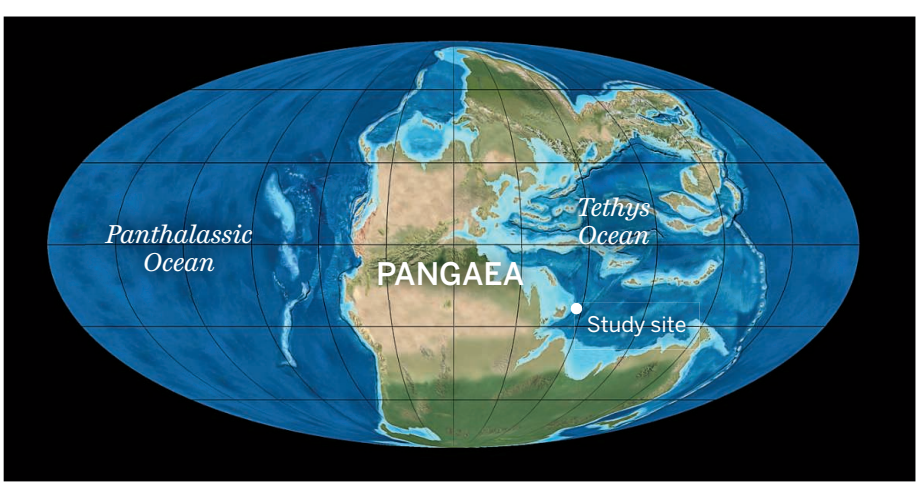

CREDITS: (PHOTO) D. ASTRATTI; (IMAGE) RON BLAKEY/COLORADO PLATEAU GEOSYSTEMS INC.

30. M. X. Kirby, B. MacFadden, *Palaeogeogr. Palaeoclimatol. Palaeoecol.* **228**, 193–202 (2005).

ACKNOWLEDGMENTS

Supported by Ecopetrol-ICP "Cronología de la Deformación en las Cuencas Subandinas," Smithsonian Institution, Uniandes P12. 160422.002/001, Autoridad del Canal de Panama (ACP), the Mark Tupper Fellowship, Ricardo Perez S.A.; NSF grant EAR 0824299 and OISE, EAR, DRL 0966884, Colciencias, and the National Geographic Society. We thank N. Hoyos, D. Villagomez, A. O'Dea, C. Bustamante, O. Montenegro, and C. Ojeda. All the data reported in this manuscript are presented in the main paper and in the supplementary materials.

SUPPLEMENTARY MATERIALS

www.sciencemag.org/content/348/6231/226/suppl/DC1
Materials and Methods
Supplementary Text
Figs. S1 to S3
Tables S1 to S5
References (*31*–*42*)

12 November 2014; accepted 2 March 2015
10.1126/science.aaa2815

EARTH HISTORY

Ocean acidification and the Permo-Triassic mass extinction

M. O. Clarkson,[1]*† S. A. Kasemann,[2] R. A. Wood,[1] T. M. Lenton,[3] S. J. Daines,[3] S. Richoz,[4] F. Ohnemueller,[2] A. Meixner,[2] S. W. Poulton,[5] E. T. Tipper[6]

Ocean acidification triggered by Siberian Trap volcanism was a possible kill mechanism for the Permo-Triassic Boundary mass extinction, but direct evidence for an acidification event is lacking. We present a high-resolution seawater pH record across this interval, using boron isotope data combined with a quantitative modeling approach. In the latest Permian, increased ocean alkalinity primed the Earth system with a low level of atmospheric CO_2 and a high ocean buffering capacity. The first phase of extinction was coincident with a slow injection of carbon into the atmosphere, and ocean pH remained stable. During the second extinction pulse, however, a rapid and large injection of carbon caused an abrupt acidification event that drove the preferential loss of heavily calcified marine biota.

The Permo-Triassic Boundary (PTB) mass extinction, at ~252 million years ago (Ma), represents the most catastrophic loss of biodiversity in geological history and played a major role in dictating the subsequent evolution of modern ecosystems (*1*). The PTB extinction event spanned ~60,000 years (*2*) and can be resolved into two distinct marine extinction pulses (*3*). The first occurred in the latest Permian [Extinction Pulse 1 (EP1)] and was followed by an interval of temporary recovery before the second pulse (EP2), which occurred in the earliest Triassic. The direct cause of the mass extinction is widely debated, with a diverse range of overlapping mechanisms proposed, including widespread water column anoxia (*4*), euxinia (*5*), global warming (*6*), and ocean acidification (*7*).

Models of PTB ocean acidification suggest that a massive and rapid release of CO_2 from Siberian Trap volcanism acidified the ocean (*7*). Indirect evidence for acidification comes from the interpretation of faunal turnover records (*3*, *8*), potential dissolution surfaces (*9*), and Ca isotope data (*7*). A rapid input of carbon is also potentially recorded in the negative carbon isotope excursion (CIE) that characterizes the PTB interval (*10*, *11*). The interpretation of these records is, however, debated (*12*–*16*) and is of great importance to understanding the current threat of anthropogenically driven ocean acidification (*11*).

To test the ocean acidification hypothesis, we have constructed a proxy record of ocean pH across the PTB using the boron isotope composition of marine carbonates ($\delta^{11}B$) (*17*). We then used a carbon cycle model (supplementary text) to explore ocean carbonate chemistry and pH scenarios that are consistent with our $\delta^{11}B$ data and published records of carbon cycle disturbance and environmental conditions. Through this combined geochemical, geological, and modeling approach, we are able to produce an envelope that encompasses the most realistic range in pH, which then allows us to resolve three distinct chronological phases of carbon cycle perturbation, each with very different environmental consequences for the Late Permian–Early Triassic Earth system.

We analyzed boron and carbon isotope data from two complementary transects in a shallow marine, open-water carbonate succession from the United Arab Emirates (U.A.E.), where depositional facies and stable carbon isotope ratio ($\delta^{13}C$) are well constrained (*18*). During the PTB interval, the U.A.E. formed an expansive carbonate platform that remained connected to the central Neo-Tethyan Ocean (Fig. 1A) (*18*). Conodont stratigraphy and the distinct $\delta^{13}C$ curve are used to constrain the age model (*17*).

The PTB in the Tethys is characterized by two negative $\delta^{13}C$ excursions interrupted by a short-term positive event (*10*). There is no consensus as to the cause of this "rebound" event and so we instead focus on the broader $\delta^{13}C$ trend. Our $\delta^{13}C$ transect (Fig. 1B) starts in the Changhsingian (Late Permian) with a gradual decreasing trend, interrupted by the first negative shift in $\delta^{13}C$ at EP1 (at 53 m, ~251.96 Ma) (Figs. 1B and 2). This is followed by the minor positive rebound event (at 54 m, ~251.95 Ma) (Figs. 1B and 2) before the minima of the second phase of the negative CIE (58 to 60 m, ~251.92 Ma) (Figs. 1B and 2) that marks the PTB itself. After the CIE minimum, $\delta^{13}C$ gradually increases to ~1.8 per mil (‰) and remains relatively stable during the earliest Triassic and across EP2.

Our boron isotope record shows a different pattern to the carbon isotope excursion. The boron isotope ratio ($\delta^{11}B$) is persistently low (Fig. 1C) at the start of our record during the late-Changhsingian, with an average of 10.9 ± 0.9‰ (1σ). This is in agreement with $\delta^{11}B$ values (average of 10.6 ± 0.6‰, 1σ) reported for early-Permian brachiopods (*19*). Further up the section (at ~40 m, ~252.04 Ma) (Fig. 1C), there is a stepped increase in $\delta^{11}B$ to 15.3 ± 0.8‰ (propagated uncertainty, 2σf) and by implication an increase in ocean pH of ~0.4 to 0.5 (Fig. 2). $\delta^{11}B$ values then remain relatively stable, scattering around 14.7 ± 1.0‰ (1σ) and implying variations within 0.1 to 0.2 pH, into the Early Griesbachian (Early Triassic) and hence across EP1 and the period of carbon cycle disturbance (Figs. 1 and 2).

After the $\delta^{13}C$ increase and stabilization (at ~85 m, ~251.88 Ma) (Fig. 1), $\delta^{11}B$ begins to decrease rapidly to 8.2 ± 1.2‰ (2σf), implying a sharp drop in pH of ~0.6 to 0.7. The $\delta^{11}B$ minimum is coincident with the interval identified as EP2. This ocean acidification event is short-lived (~10,000 years), and $\delta^{11}B$ values quickly recover toward the more alkaline values evident during EP1 (average of ~14‰).

The initial rise in ocean pH of ~0.4 to 0.5 units during the Late Permian (Fig. 2) suggests a large increase in carbonate alkalinity (*20*). We are able to simulate the observed rise in $\delta^{11}B$ and pH through different model combinations of increasing silicate weathering, increased pyrite deposition (*21*), an increase in carbonate weathering, and a decrease in shallow marine carbonate depositional area (supplementary text). Both silicate weathering and pyrite deposition result in a large drop in partial pressure of CO_2 (P_{CO_2}) (and temperature) for a given increase in pH and saturation state (Ω). There is no evidence for a large drop in P_{CO_2}, and independent proxy data

[1]School of Geosciences, University of Edinburgh, West Mains Road, Edinburgh EH9 3FE, UK. [2]Faculty of Geosciences and MARUM–Center for Marine Environmental Sciences, University of Bremen, 28334 Bremen, Germany. [3]College of Life and Environmental Sciences, University of Exeter, Laver Building, North Parks Road, Exeter EX4 4QE, UK. [4]Institute of Earth Sciences, NAWI Graz, University of Graz, Heinrichstraße 26, 8010 Graz, Austria. [5]School of Earth and Environment, University of Leeds, Leeds LS2 9JT, UK. [6]Department of Earth Sciences, University of Cambridge, Downing Street, Cambridge CB2 3EQ, UK.
*Corresponding author. E-mail: matthew.clarkson@otago.ac.nz
†Present address: Department of Chemistry, University of Otago, Union Street, Dunedin, 9016, Post Office Box 56, New Zealand.

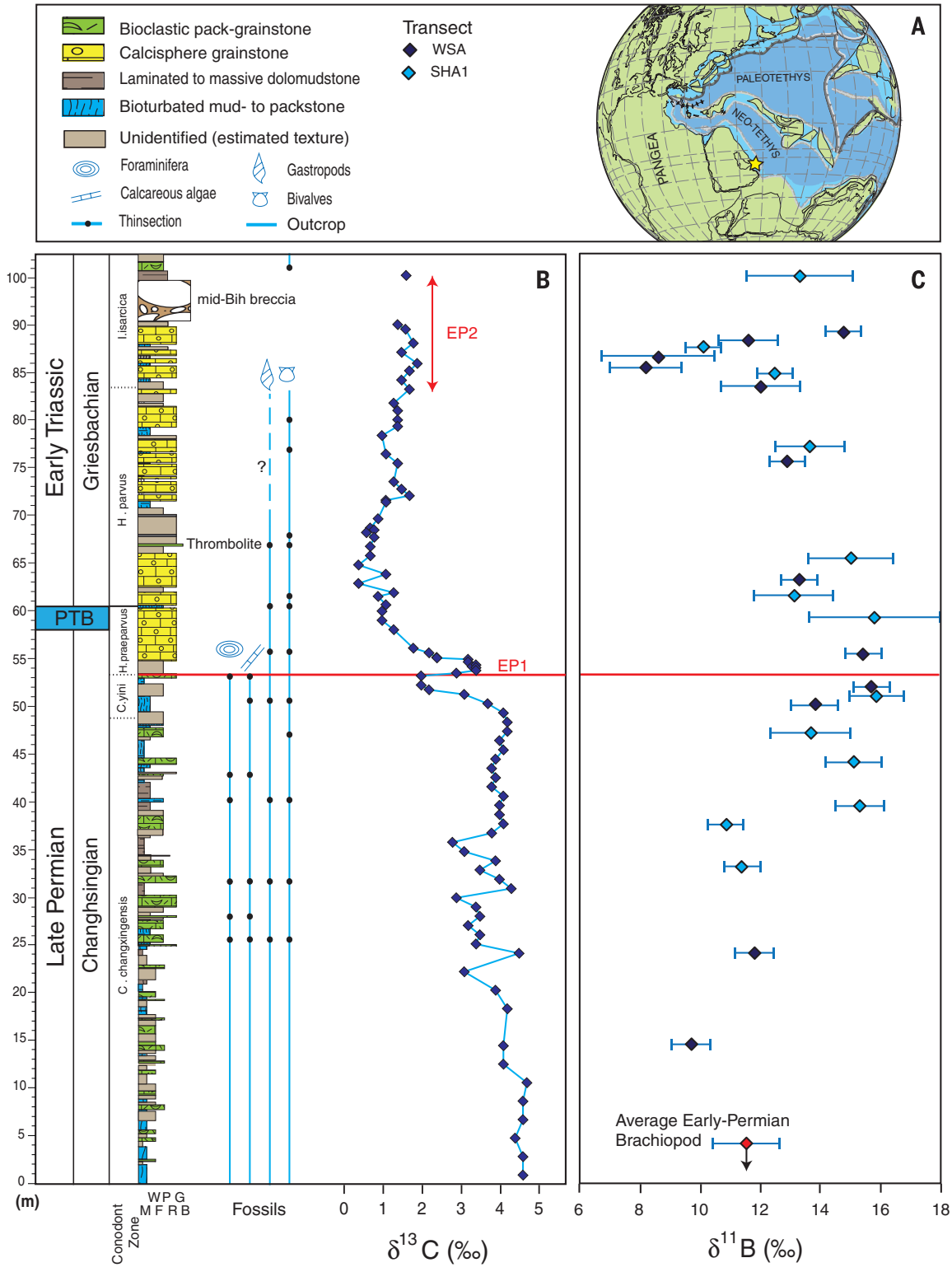

Fig. 1. Site locality and high-resolution carbon and boron isotope data. (**A**) Paleogeographic reconstruction for the Late Permian showing the studied section Wadi Bih, in the Musandam Mountains of U.A.E., that formed an extensive carbonate platform in the Neo-Tethyan Ocean. [Modified from (*35*).] (**B**) Shallow water $\delta^{13}C$ record (*18*). (**C**) Boron isotope ($\delta^{11}B$) record (propagated uncertainty given as $2\sigma_f$) and average Early Permian brachiopod value (n = 5 samples) (*19*). Lithology, biota, and transect key are provided in (A). Only *Hindeodus parvus* has been found so far in this section (*18*), and the conodont zones with dashed lines are identified from the $\delta^{13}C$ record and regional stratigraphy (*36*–*38*).

indicate only a minor temperature decrease of a few degrees celsius during the Changhsingian (*22*), suggesting that these mechanisms alone cannot explain the pH increase (fig. S5). Conversely, an increase in carbonate input or a reduction in rates of carbonate deposition both result in increases in Ω, with a greater impact on pH per unit decrease in P_{CO_2} and temperature (fig. S6).

A decrease in carbonate sedimentation is consistent with the decrease in depositional shelf area that occurred because of the second-order regression of the Late Permian (*23*). With the added expansion of anoxia into shelf environments (*24*), this would effectively create both bottom-up and top-down pressures to reduce the area of potential carbonate sedimentation.

Sea-level fall also exposed carbonates to weathering (*23*), which would have further augmented the alkalinity influx. The pH increase event supports the CO_2*Lo* initialization scenario [CO_2 ~3 present atmospheric levels (PAL), pH ~8, $\delta^{11}B_{SW}$ ~34‰] (supplementary text) because the simulated CO_2 and temperature decrease is much reduced and therefore is more consistent with

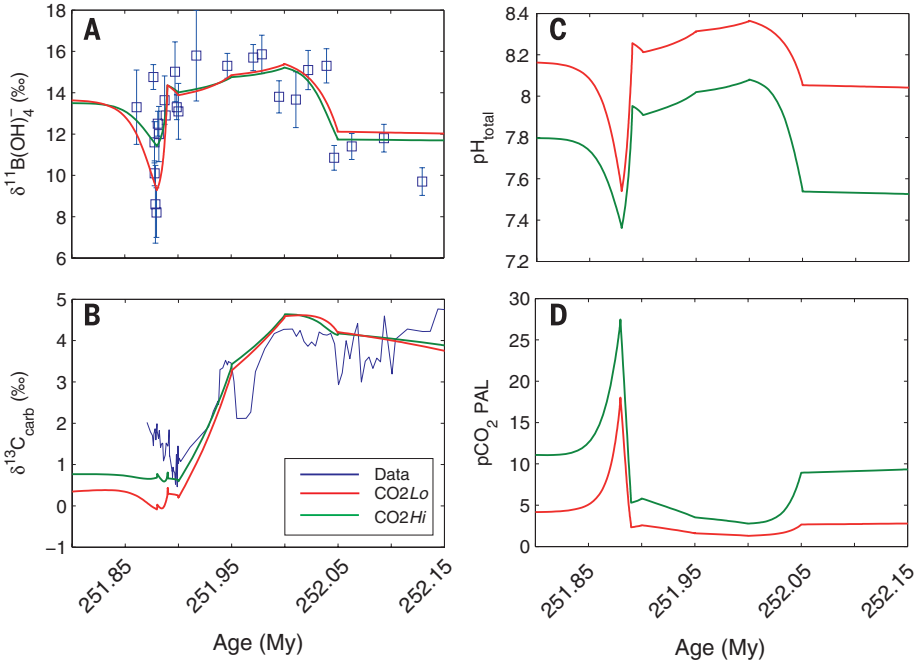

Fig. 2. Model results of carbon cycle parameters for high- and low-CO_2 end-member scenarios. (**A**) Model-reproduced $\delta^{11}B$ versus data. (**B**) Modeled $\delta^{13}C$ versus data. (**C**) Modeled pH envelope incorporating uncertainty of seawater B isotope composition ($\delta^{11}B_{SW}$) and dynamic temperatures. (**D**) Calculated atmospheric CO_2.

independent proxy data (*22*), as compared with CO_2*Hi* (CO_2 ~10 PAL, pH ~7.5, $\delta^{11}B_{SW}$ ~36.8‰) (Fig. 2D).

Before EP1, $\delta^{13}C_{carb}$ values began to decrease before reaching the minimum of the globally recognized negative CIE at the PTB (Fig. 1). At this time, both $\delta^{11}B$ and ocean pH remained stable. Hypotheses to explain the negative CIE require the input of isotopically light carbon, such as from volcanism (*14*, *25*), with the assimilation of very light organic carbon from the surrounding host rock (*26*), methane destabilization (*27*), collapse of the biological pump (*15*), and/or a decrease in the burial of terrestrial carbon (*16*). We can simulate the observed drop in $\delta^{13}C$, while remaining within the uncertainty of the $\delta^{11}B$ data (Fig. 2), by combining a cessation of terrestrial carbon burial with a relatively slow (50,000 years) carbon injection from any of the above sources (fig. S8). A small source of methane (3.2×10^{17} mol C with $\delta^{13}C = -50‰$) gives the least change in $\delta^{11}B$ and pH, whereas either a larger source of organic carbon (~6.5×10^{17} mol C with $\delta^{13}C = -25‰$) or a mixture of mantle and lighter carbon sources (~1.3×10^{18} mol C with $\delta^{13}C = -12.5‰$) are still within the measured uncertainty in $\delta^{11}B$.

This relatively slow addition of carbon minimizes the tendency for a transient decline in surface ocean pH in an ocean that was already primed with a high Ω and hence high buffering capacity from the Late Permian. The global presence of microbial and abiotic carbonate fabrics after EP1 (*28*) is indicative that this high Ω was maintained across the CIE. The carbon injection triggers an increase in P_{CO_2}, temperature, and silicate weathering, creating an additional counterbalancing alkalinity flux, which is consistent with independent proxy data (*6*). The alkalinity source may have been further increased through soil loss (*29*), the emplacement of easily weathered Siberian Trap basalt, or the impact of acid rain (*30*), which would have increased weathering efficiency.

The negative $\delta^{11}B_{carb}$ excursion at 251.88 Ma represents a calculated pH decrease of up to 0.7 pH. This pH decrease coincides with the second pulse of the extinction (Fig. 1), which preferentially affected the heavily calcifying, physiologically unbuffered, and sessile organisms (*3*). This was also accompanied by the temporary loss of abiotic and microbial carbonates throughout the Tethys (*31*, *32*), suggesting a coeval decrease in Ω. To overwhelm the buffering capacity of the ocean and decrease pH in this way requires a second, more abrupt injection of carbon into the atmosphere, yet remarkably, the acidification event occurs after the decline in $\delta^{13}C$, when $\delta^{13}C$ has rebounded somewhat and is essentially stable (Fig. 1).

Unlike the first carbon injection, the lack of change in $\delta^{13}C$ at this time rules out very ^{13}C-depleted carbon sources because no counterbalancing strongly ^{13}C-enriched source exists. Instead, it requires a carbon source near ~0‰. A plausible scenario for this is the decarbonation of overlying carbonate host rock, into which the Siberian Traps intruded (*26*), or the direct assimilation of carbonates and evaporites into the melt (*33*). Host carbonates would have had $\delta^{13}C$ ~ +2 to 4‰, which when mixed with mantle carbon (~−5‰) potentially produces a source near 0‰. We can simulate the sharp drop in pH and stable $\delta^{13}C$ values (Fig. 2) through a large and rapid carbon release of 2×10^{18} mol C over 10,000 years (fig. S8). This is undoubtedly a massive injection of 24,000 PgC at a rapid rate of 2.4 PgC/year, but it is physically plausible given existing estimates of the volume of carbonate host sediments subject to contact metamorphism and postulated mechanisms of carbon release (supplementary text). This second rapid carbon release produces a sharp rise in P_{CO_2} to ~20 PAL and warming of ~15°C, which is consistent with the observation of peak temperatures after EP1 (*22*). Initialization of the carbon cycle model under CO_2*Hi* cannot generate the magnitude of $\delta^{11}B$ drop (Fig. 2A) because the nonlinear relation between pH and $\delta^{11}B$ fractionation sets a lower limit of $\delta^{11}B$ at ~10‰ in this case (fig. S3). Thus, low initial CO_2 of ~3 PAL in the Late Permian (CO_2*Lo*) is more consistent with our data.

An acidification event of ~10,000 years is consistent with the modeled time scale required to replenish the ocean with alkalinity, as carbonate deposition is reduced and weathering is increased under higher P_{CO_2} and global temperatures. Increased silicate weathering rates drive further CO_2 drawdown, resulting in stabilization (Fig. 2D). High global temperature (*6*) and increased silicate weathering are consistent with a sudden increase in both $^{87}Sr/^{86}Sr$ (*34*) and sedimentation rates (*29*) in the Griesbachian.

The PTB was a time of extreme environmental change, and our combined data and modeling approach falsifies several of the mechanisms currently proposed. Although the coincident stresses of anoxia, increasing temperature, and ecosystem restructuring were important during this interval, the $\delta^{11}B$ record strongly suggests that widespread ocean acidification was not a factor in the first phase of the mass extinction but did drive the second pulse. The carbon release required to drive the observed acidification event must have occurred at a rate comparable with the current anthropogenic perturbation but exceeds it in expected magnitude. Specifically, the required model perturbation of 24,000 PgC exceeds the ~5000 PgC of conventional fossil fuels and is at the upper end of the range of estimates of unconventional fossil fuels (such as methane hydrates). We show that such a rapid and large release of carbon is critical to causing the combined synchronous decrease in both pH and saturation state that defines an ocean acidification event (*11*).

REFERENCES AND NOTES

1. D. H. Erwin, *Nature* **367**, 231–236 (1994).
2. S. D. Burgess, S. Bowring, S. Z. Shen, *Proc. Natl. Acad. Sci. U.S.A.* **111**, 3316–3321 (2014).
3. H. J. Song, P. B. Wignall, J. A. Tong, Y. Hongfu, *Nat. Geosci.* **6**, 52–56 (2012).
4. P. B. Wignall, R. J. Twitchett, *Science* **272**, 1155–1158 (1996).
5. K. Grice *et al.*, *Science* **307**, 706–709 (2005).
6. Y. Sun *et al.*, *Science* **338**, 366–370 (2012).
7. J. L. Payne *et al.*, *Proc. Natl. Acad. Sci. U.S.A.* **107**, 8543–8548 (2010).
8. A. H. Knoll, R. K. Barnbach, J. L. Payne, S. Pruss, W. W. Fischer, *Earth Planet. Sci. Lett.* **256**, 295–313 (2007).
9. J. L. Payne *et al.*, *Geol. Soc. Am. Bull.* **119**, 771–784 (2007).
10. C. Korte, H. W. Kozur, *J. Asian Earth Sci.* **39**, 215–235 (2010).

11. B. Hönisch *et al.*, *Science* **335**, 1058–1063 (2012).
12. C. L. Blättler, H. C. Jenkyns, L. M. Reynard, G. M. Henderson, *Earth Planet. Sci. Lett.* **309**, 77–88 (2011).
13. P. B. Wignall, S. Kershaw, P. Y. Collin, S. Crasquin-Soleau, *Geol. Soc. Am. Bull.* **121**, 954–956 (2009).
14. R. A. Berner, *Proc. Natl. Acad. Sci. U.S.A.* **99**, 4172–4177 (2002).
15. M. R. Rampino, K. Caldeira, *Terra Nova* **17**, 554–559 (2005).
16. W. S. Broecker, S. Peacock, *Global Biogeochem. Cycles* **13**, 1167–1172 (1999).
17. Materials and methods are available on *Science* Online
18. M. O. Clarkson *et al.*, *Gondwana Res.* **24**, 233–242 (2013).
19. M. M. Joachimski, L. Simon, R. van Geldern, C. Lecuyer, *Geochim. Cosmochim. Acta* **69**, 4035–4044 (2005).
20. The alternative way to drive an increase in pH would be through a removal of carbon; however, this would be evident in the $\delta^{13}C$ record, so we can rule it out.
21. Bacterial sulfate reduction (BSR) is a net source of alkalinity if the generated H_2S is buried as pyrite. Pyrite deposition is seen widely in certain settings during the Late Permian to PTB. Further information is provided in the supplementary materials.
22. M. M. Joachimski *et al.*, *Geology* **40**, 195–198 (2012).
23. H. Yin *et al.*, *Earth Sci. Rev.* **137**, 19–33 (2014).
24. P. B. Wignall, R. J. Twitchett, in *Catastrophic Events and Mass Extinctions: Impacts and Beyond*, C. Koeberl, K. G. MacLeod, Eds. (Geological Society of America, Boulder, CO, 2002), pp. 395–413.
25. C. Korte *et al.*, *J. Asian Earth Sci.* **37**, 293–311 (2010).
26. H. Svensen *et al.*, *Earth Planet. Sci. Lett.* **277**, 490–500 (2009).
27. E. S. Krull, G. J. Retallack, *Geol. Soc. Am. Bull.* **112**, 1459–1472 (2000).
28. A. D. Woods, *Earth Sci. Rev.* **137**, 6–18 (2013).
29. T. J. Algeo, Z. Q. Chen, M. L. Fraiser, R. J. Twitchett, *Palaeogeogr. Palaeoclimatol. Palaeoecol.* **308**, 1–11 (2011).
30. B. A. Black, J. F. Lamarque, C. A. Shields, L. T. Elkins-Tanton, J. T. Kiehl, *Geology* **42**, 67–70 (2014).
31. A. Baud, S. Richoz, S. Pruss, *Global Planet. Change* **55**, 81–89 (2007).
32. S. Richoz *et al.*, *J. Asian Earth Sci.* **39**, 236–253 (2010).
33. B. A. Black, L. T. Elkins-Tanton, M. C. Rowe, I. U. Peate, *Earth Planet. Sci. Lett.* **317**, 363–373 (2012).
34. C. Korte *et al.*, *Int. J. Earth Sci.* **93**, 565–581 (2004).
35. G. M. Stampfli, G. D. Borel, *Earth Planet. Sci. Lett.* **196**, 17–33 (2002).
36. S. Z. Shen *et al.*, *Earth Planet. Sci. Lett.* **375**, 156–165 (2013).
37. B. Koehrer *et al.*, *GeoArabia* **15**, 91–156 (2010).
38. F. Maurer, R. Martini, R. Rettori, H. Hillgartner, S. Cirilli, *GeoArabia* **14**, 125–158 (2009).

ACKNOWLEDGMENTS

M.O.C. acknowledges funding from the Edinburgh University Principal's Career Development Scholarship, the International Centre for Carbonate Reservoirs, and The Marsden Fund (U001314). R.A.W., T.M.L., and S.W.P. acknowledge support from the Natural Environment Research Council through the "Co-evolution of Life and the Planet" scheme (NE/I005978). T.M.L. and S.J.D. were supported by the Leverhulme Trust (RPG-2013-106). S.A.K. and A.M. acknowledge support from the German Research Foundation (Deutsche Forschungsgemeinschaft) Major Research Instrumentation Program INST 144/307-1. This is a contribution to IGCP 572, with S.R. sponsored for fieldwork by the Austrian National Committee (Austrian Academy of Sciences) for the International Geoscience Programme (IGCP). We are grateful to R. Newton and A. Thomas for helpful discussions, L. Krystyn for field assistance, F. Maurer for discussions on stratigraphy and providing photomicrographs, and B. Mills for assisting with model studies. Data are available online in the supplementary materials and at www.pangaea.de.

SUPPLEMENTARY MATERIALS

www.sciencemag.org/content/348/6231/229/suppl/DC1
Materials and Methods
Supplementary Text
Figs. S1 to S9
Tables S1 to S10
References (*39*–*98*)

8 October 2014; accepted 4 March 2015
10.1126/science.aaa0193

COMETARY FORMATION

Molecular nitrogen in comet 67P/Churyumov-Gerasimenko indicates a low formation temperature

M. Rubin,[1]* K. Altwegg,[1,2] H. Balsiger,[1] A. Bar-Nun,[3] J.-J. Berthelier,[4] A. Bieler,[1,5] P. Bochsler,[1] C. Briois,[6] U. Calmonte,[1] M. Combi,[5] J. De Keyser,[7] F. Dhooghe,[7] P. Eberhardt,[1]† B. Fiethe,[8] S. A. Fuselier,[9] S. Gasc,[1] T. I. Gombosi,[5] K. C. Hansen,[5] M. Hässig,[1,9] A. Jäckel,[1] E. Kopp,[1] A. Korth,[10] L. Le Roy,[2] U. Mall,[10] B. Marty,[11] O. Mousis,[12] T. Owen,[13] H. Rème,[14,15] T. Sémon,[1] C.-Y. Tzou,[1] J. H. Waite,[9] P. Wurz[1]

Molecular nitrogen (N_2) is thought to have been the most abundant form of nitrogen in the protosolar nebula. It is the main N-bearing molecule in the atmospheres of Pluto and Triton and probably the main nitrogen reservoir from which the giant planets formed. Yet in comets, often considered the most primitive bodies in the solar system, N_2 has not been detected. Here we report the direct in situ measurement of N_2 in the Jupiter family comet 67P/Churyumov-Gerasimenko, made by the Rosetta Orbiter Spectrometer for Ion and Neutral Analysis mass spectrometer aboard the Rosetta spacecraft. A N_2/CO ratio of $(5.70 \pm 0.66) \times 10^{-3}$ (2σ standard deviation of the sampled mean) corresponds to depletion by a factor of ~25.4 ± 8.9 as compared to the protosolar value. This depletion suggests that cometary grains formed at low-temperature conditions below ~30 kelvin.

Thermochemical models of the protosolar nebula (PSN) suggest that molecular nitrogen (N_2) was the principal nitrogen species during the disk phase (*1*) and that the nitrogen present in the giant planets was accreted in this form (*2*). Moreover, Pluto and Triton, which are both expected to have formed in the same region of the PSN as Jupiter family comets (JFCs), have N_2-dominated atmospheres and surface deposits of N_2 ice (*3*, *4*). This molecule has never been firmly detected in comets; however, CN, HCN, NH, NH_2, and NH_3 among others have been observed spectroscopically (*5*, *6*). The abundance of N_2 in comets is therefore a key to understanding the conditions in which they formed.

Condensation or trapping of N_2 in ice occurs at similar thermodynamic conditions as those needed for CO in the PSN (*7*, *8*). This requires very low PSN temperatures and implies that the detection of N_2 in comets and its abundance ratio with respect to CO would put strong constraints on comet formation conditions (*7*, *8*). Ground-based spectroscopic observations of the N_2^+ band in the near ultraviolet are very difficult because of the presence of telluric N_2^+ and other cometary emission lines. Searches conducted with high-resolution spectra of comets 122P/de Vico, C/1995 O1 (Hale-Bopp), and 153P/2002 C1 (Ikeya-Zhang) have been unsuccessful and yielded upper limits of 10^{-5} to 10^{-4} for the N_2^+/CO^+ ratio (*9*, *10*). Only one N_2^+ detection in C/2002 VQ94 (LINEAR) from ground-based observations is convincing, because the comet was at sufficient distance from the Sun to prevent terrestrial twilight N_2^+ contamination (*11*). The in situ measurements made by Giotto in 1P/Halley were inconclusive, because the resolution of the mass spectrometers aboard the spacecraft (*12*) was insufficient to separate the nearly identical masses of N_2 and CO during the 1P/Halley encounter, and only an upper limit could be derived for the relative production rates $[Q(N_2)/Q(CO) \leq 0.1]$ (*13*).

Here we report the direct in situ measurement of the N_2/CO ratio by the Rosetta Orbiter Spectrometer for Ion and Neutral Analysis (ROSINA)

[1]Physikalisches Institut, University of Bern, Sidlerstrasse 5, CH-3012 Bern, Switzerland. [2]Center for Space and Habitability, University of Bern, Sidlerstrasse. 5, CH-3012 Bern, Switzerland. [3]Department of Geoscience, Tel-Aviv University, Ramat-Aviv, Tel-Aviv, Israel. [4]Laboratoire Atmosphères, Milieux, Observations Spatiales (LATMOS)/Institute Pierre Simon Laplace–CNRS-UPMC-UVSQ, 4 Avenue de Neptune F-94100, Saint-Maur, France. [5]Department of Atmospheric, Oceanic and Space Sciences, University of Michigan, 2455 Hayward, Ann Arbor, MI 48109, USA. [6]Laboratoire de Physique et Chimie de l'Environnement et de l'Espace (LPC2E), UMR 6115 CNRS–Université d'Orléans, Orléans, France. [7]Belgian Institute for Space Aeronomy, Belgisch Instituut voor Ruimte-Aeronomie–Institut d'Aéronomie Spatiale de Belgique (BIRA-IASB), Ringlaan 3, B-1180 Brussels, Belgium. [8]Institute of Computer and Network Engineering, Technische Universität Braunschweig, Hans-Sommer-Straße 66, D-38106 Braunschweig, Germany. [9]Department of Space Science, Southwest Research Institute, 6220 Culebra Road, San Antonio, TX 78228, USA. [10]Max-Planck-Institut für Sonnensystemforschung, Justus-von-Liebig-Weg 3, 37077 Göttingen, Germany. [11]Centre de Recherches Pétrographiques et Géochimiques (CRPG)–CNRS, Université de Lorraine, 15 rue Notre Dame des Pauvres, Bôite Postale 20, 54501 Vandoeuvre lès Nancy, France. [12]Aix Marseille Université, CNRS, Laboratoire d'Astrophysique de Marseille UMR 7326, 13388, Marseille, France. [13]Institute for Astronomy, University of Hawaii, Honolulu, HI 96822, USA. [14]Université de Toulouse; UPS-OMP; Institut de Recherche en Astrophysique et Planétologie (IRAP), Toulouse, France. [15]CNRS; IRAP; 9 Avenue du Colonel Roche, Boîte Postale 44346, F-31028 Toulouse Cedex 4, France.
*Corresponding author. E-mail: martin.rubin@space.unibe.ch
†Deceased.

Ocean acidification and the Permo-Triassic mass extinction
M. O. Clarkson *et al.*
Science **348**, 229 (2015);
DOI: 10.1126/science.aaa0193